C. R. Mecanique 339 (2011) 552–562

Contents lists available at ScienceDirect

Comptes Rendus Mecanique

www.sciencedirect.com

Surface mechanics: facts and numerical models

Investigation of mechanically attrited structures induced by repeated impacts on an AISI1045 steel

Guillaume Kermouche [a,*], Guillaume Pacquaut [a], C. Langlade [b], Jean-Michel Bergheau [a]

[a] *Université de Lyon, ENISE, LTDS, UMR CNRS 5513, 42023 Saint-Etienne, France*
[b] *Université technologique de Belfort-Montbeliard, LERMPS EA 3316, 90010 Belfort cedex, France*

ARTICLE INFO

Article history:
Available online 21 June 2011

Keywords:
Fatigue
Mechanically attrited structures
AISI1045 steel

ABSTRACT

Under repeated impact loadings – shot peening process, surface mechanical attrition treatment, erosive wear – metallic surfaces undergo severe plastic deformation which leads sometimes to a local change of their microstructure. These mechanically attrited structures (MAS) exhibit very interesting physical properties: high hardness, better tribological properties, etc. Consequently it is of primary importance to understand the mechanism explaining how these MAS are created and grow under such loadings. In this article, this mechanism is investigated with the help of a coupled experimental and finite element approach. First, the MAS are generated on an AISI1045 steel with a micro-impact tester which allows to know the impact energy and the location of impacts with a very good accuracy. The evolution of the MAS shape as a function of the impact number is presented. Then, the finite element investigation is presented. It is shown that a macroscopic stabilized elastic regime is reached after one hundred impacts. It also appears that a close cycle of plastic strain is observed locally in the zone where material transformation should happen during this regime. The severe plastic deformation achieved after a given number of cycles may thus explain the material transformation. Based on these results, we propose a mechanism based on a plastic strain threshold to explain the growth of the MAS. The resulting MAS size and shape appear to be in very good agreement with the experimental results. Finally, we conclude on the influence of the mechanical parameters that are involved in the proposed mechanism.

1. Introduction

Resistance to wear, fatigue or corrosion of materials is strongly linked to the microstructure and properties of material surfaces. Hence, the control and the optimization of the surface microstructure and properties may improve in a significant way the service lifetime of materials. For example, it has been evidenced during the past ten years that nanocrystalline surface layers exhibit properties that are fundamentally different from their conventional polycrystalline counterparts, such as high hardness and better tribological properties [1–10]. One way to obtain nanocrystalline layer is to deposit appropriate coatings on the surface. In this case, the predominant factor is the bond between the coating and the substrate. One other way is to transform the original coarse-grained surface layer of a given bulk material into nano-sized grains. Indeed, the key point for realizing such superficial structures is to introduce in the bulk material a large amount of defects so that its microstructures are transformed into nano-sized crystallites. Hence, processes creating severe plastic deformation near the material surface may lead to the generation of a nanostructured surface layer [3–10].

---

* Corresponding author.
E-mail address: kermouche@enise.fr (G. Kermouche).

1631-0721/$ – see front matter © 2011 Académie des sciences. Published by Elsevier Masson SAS. All rights reserved.
doi:10.1016/j.crme.2011.05.012

Such nanocrystalline structures have been evidenced and characterized in several tribological systems like the white phase (WP) in ball bearing applications [2], the tribologically transformed structure (TTS) in fretting wear [3] or the mechanically mixed layer (MML) in sliding wear cases [11]. Sauger et al. [3] proposed that fretting TTS results from a recrystallization phenomenon. The transformed structure is induced by severe plastic deformation which leads to the nucleation and the growth of new grains close to the initial grain boundaries, and thus to such fine nanostructures. Rigney et al. [11] considered that the creation of MML during sliding contact was intrinsically linked to the presence of high plastic strains together with particles transfer phenomena. The particles are deformed under the action of each impact and are mixed with those of the initial material and with the oxide particles located at the surface of the workpiece. The authors called such a structure a “mechanically mixed layer”, thanks to its analogous origin with mechanical alloying [12]. This model introduces a second phase, which is necessary for generating very fine grains. Busquet et al. [10] have investigated the formation of Mechanically Modified Superficial Structures (M2S2) on two carbon steels – AISI1005, AISI1045 – with the help of a Bridgman Anvil apparatus which allows shearing samples in torsion under pressures. They have particularly shown that these superficial structures could be associated with strong equivalent plastic strain values and strong hydrostatic pressure. Moreover they also noticed that a large strain gradient is necessary to activate the grain refinement process with such loading. Let us note that many terms have been used to define these superficial nanocrystalline structures: Tribologically Transformed Structure (TTS), White Phase (WP), Mechanically Mixed Layer (MML), etc. It is difficult to state which definition is the appropriate one. For that purpose, Busquet et al. [10] have proposed to describe any kind of near-surface layer structural modifications obtained under tribological conditions by the terms “Mechanically Modified Superficial Structures (M2S2)”.

As shown by Lu and coworkers [6–9], repeated multi-directional impacts may also result in severe plastic deformation of metallic surfaces which may lead to grain refinement. From this observation, they have developed a new technique, namely “Surface Mechanical Attrition Treatment”, which is based on the peening of multiple balls to the surface. During the treatment, the sample is peened by a large number of shots in a short period of time. The mechanism of surface nanocrystallization during the SMAT process has been widely investigated during the past ten years by these authors. For example, in materials having high stacking fault energy such as pure iron, dislocation wall and cells are formed in order to accommodate plastic strain. At a certain strain level, for minimizing the total system energy, the dislocation walls are transformed into sub-boundaries which lead to grain refinement. With further straining, the dislocation walls are formed inside the inner of the refined grains and these refined grains are further subdivided following a similar mechanism. The strain rate role plays also an important role in the grain refinement process because, at a given level of strain, the dislocation density increases with an increasing strain rate. Dislocation activity being temperature sensitive, lower temperature may also enhance grain refinement [6,7]. In materials having low stacking fault energy such as the AISI304 stainless steel, the refinement process is a bit different. It involves formation of planar dislocation arrays and twins then intersection of multi-directional twins leading to grain subdivisions and martensite transformation. Here again this process is enhanced by the combination of large plastic strains and high strain rates [6,8,9]. Let us note that in the SMAT process, it is difficult to state if these transformations are linked or not to the tribological conditions, hence the terms M2S2 may not be adapted. For that purpose, we propose to the following term: Mechanically Attrited Structure (MAS).

Sekkal et al. [1] have also investigated the creation of mechanically attrited structures under localized repeated normal impact loadings using a micro-impact tester on a Ti6Al4V titanium alloy. The main difference with SMAT is that here, the impact location is totally controlled as well as the impact energy and the impact angle. Let us note that the use of such micro-impact tester may thus give important information on the relation between impact conditions and growth of nanocrystalline layer during SMA treatment. They have identified two impact regimes: an elastoplastic regime during which the impact energy is dissipated in the elastic–plastic deformation of the material followed by an elastic regime during which the impact energy is totally converted into elastic energy. This elastic regime appears after one hundred impacts. One important point in their study is that the MAS grows during the macroscopic elastic regime. It thus appears in contradiction with the usual interpretation of MAS formations based on severe plastic deformation.

The aim of this present work is to investigate the mechanical phenomena that may lead to the initiation and growth of MAS under localized repeated normal impact loadings. For that purpose a finite element analysis, specially developed to model high number repeated normal experiments, has been used. The input parameters of the FEA are based on an experimental study on an AISI1045 steel. It is shown that a close cycle of plastic strain is induced locally in the zone where material transformation should happen during the stabilized impact regime (elastic–plastic shakedown). Similarly to the SMAT, the severe plastic deformation achieved after a given number of cycles may thus explain such material transformation. We also present a mechanism aiming to describe the growth of the Mechanically Attrited Structure (MAS). The obtained MAS size and shape appear to be in good agreement with the previous experimental results.

2. Experimental results on an AISI1045 steel

Micro-impact tests with energy control have been performed using the impact tester developed in the LERMPS laboratory [13,14]. A rigid conical indenter, ended by a hemispherical tip electromagnetically accelerated is pushed onto the sample surface under normal incidence. A constant acceleration being generated by the electromagnets, the indenter velocity and kinetic energy just before the impact may be directly determined using the indenter weight and its initial position above the sample surface. The impacting tip is a Tungsten carbide cone with a semi-angle of 30° and a round apex of radius

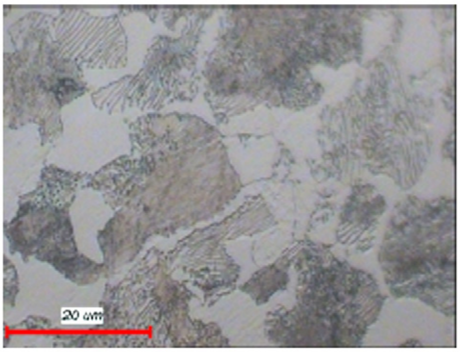

Fig. 1. Initial microstructure of the AISI1045 steel.

Table 1
Impact test parameters.

Parameters	Value
Tip radius	450 µm
Impact energy	4 mJ
Impact frequency	20 Hz
Hardness of AISI1045	200 Hv
Grain size of AISI1045	20 µm

450 µm. The impact energy is about 4 mJ and the impact frequency is 20 Hz. The impacts have been performed on a pearlitic AISI1045 steel. The grain size is about 20 µm (Fig. 1) and the hardness is about 200 Hv. The samples have been carefully polished before experiments. These impact conditions and material properties are summarized in Table 1.

Series of 500, 1000, 2000, 3000, ..., 8000 impacts have been realized. Then samples have been cross-sectioned, polished and etched. The corresponding optical micrographs are shown in Fig. 2. After etching, surface observation of the indent reveals the presence of a new microstructure, easily distinguishable from the matrix. This zone that reacts differently under etching corresponds to a Mechanically Attrited Structure (MAS). The presence of an MAS is first noticed after 500 impacts. The attrited structure is located under the surface in the center of the contact area. Scanning electron microscopy of the impact affected zone has also been performed after 5000 repeated impacts. The samples have been examined using the backscattering mode which allows to distinguish the various affected area. Here again, one may observe a good agreement between the results of Sekkal et al. [1] and the present result. Indeed, the MAS has a filament-like aspect. The zones between filaments are highly deformed and micro-cracks may be observed at the interface between filaments and the deformed area. Consequently this attrited structure should be hard and brittle, which may involve the detachment of particles when submitted to non-normal impacts [5]. Three different zones can be clearly identified: a first zone which corresponds to the MAS, a second zone which corresponds to a highly cold hardened volume and a third zone which is the remaining plastic deformed volume. As shown in Fig. 2 the size of the mechanically attrited structure depends on the number of impact. The thickness of this transformed volume ranges from 80 µm for 500 cycles to 300 µm for 5000–6000 cycles and remains constant after. The kinetics of the attrited structure growth is plotted in Fig. 3.

3. Finite element model

3.1. First attempt: explicit thermomechanical analysis

The first attempt to model the repeated normal impact experiment has been performed using the Abaqus explicit software [15]. This software is well adapted to the modeling of fast non-linear dynamic problems with coupled thermomechanical phenomena. Nevertheless, the time step in such analysis has to be small enough to maintain stability of the solution procedure. Consequently a high number of impacts cannot be modeled with this software. In order to improve the clarity of the paper, only the main results are detailed here. Let us note that the Johnson and Cook law [16] has been chosen to model the behavior of the material and the proportion of plastic work dissipated under thermal form is taken to be about 90%. It appeared that after 20 impacts, the stabilized impact regime was not reached (at each impact, there is an increase of the contact area). The evolution of the maximum temperature in the workpiece at each impact is plotted in Fig. 4. Obviously, it is maximum during the first impact where the plastic strain rate is also maximum. Nevertheless the temperature rise is not higher than 80 °C and is thus not high enough to lead alone to recrystallization phenomena. In the present study, attrition seems to originate from mechanisms other than high temperature rises. These different results point out that the attrition is a consequence of severe deformation induced by the repeated impact tests. Thus it requires a finite element model, which allows to simulate a high number of impacts.

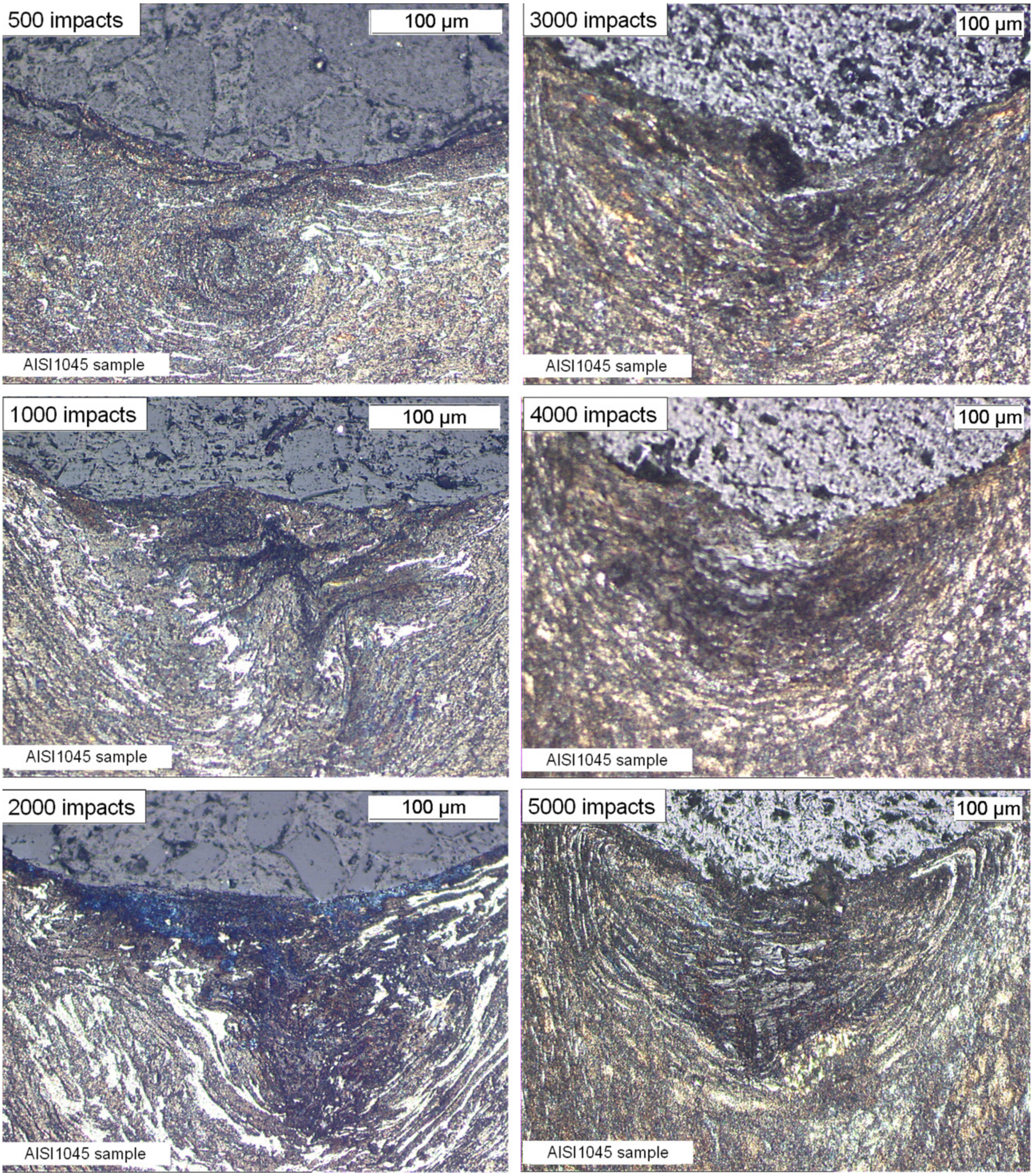

Fig. 2. Cross-sectional view of impact indents after different impact number. The presence of a new microstructure, that reacts differently under etching, corresponds to a Mechanically Attrited Structure (MAS).

3.2. A finite element model designed for repeated normal impact experiments

In order to simulate a high number of impacts, we have chosen to use a quasi-static implicit finite element analysis. Hence the stability of the solution procedure does not depend on the time step and the computation of the stress and plastic strain field is more accurate. A quasi-static approach can be used to model impact loading if and only if there is

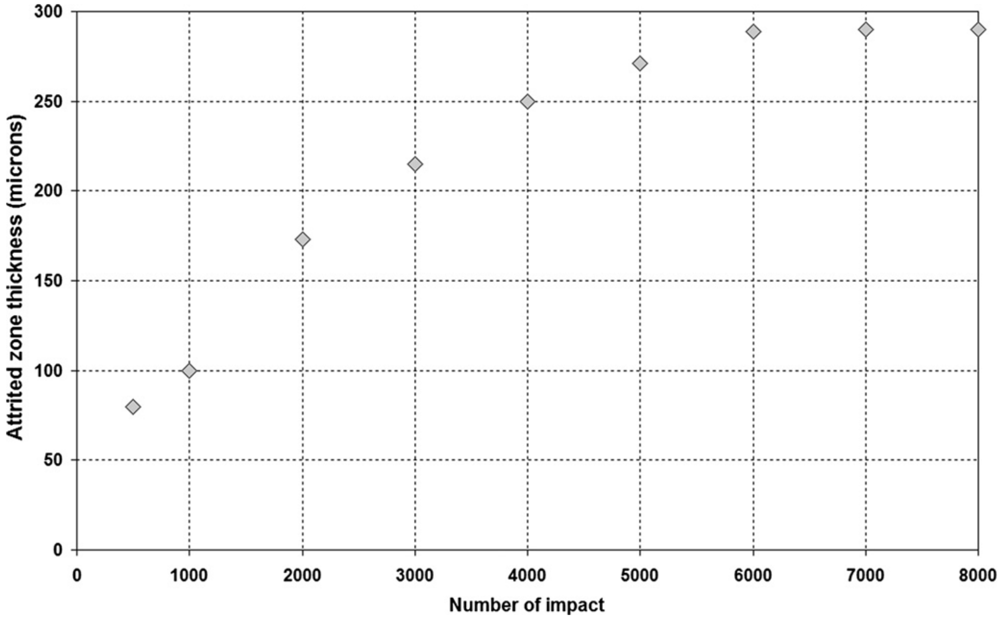

Fig. 3. Evolution of the MAS thickness as a function of the number of impacts.

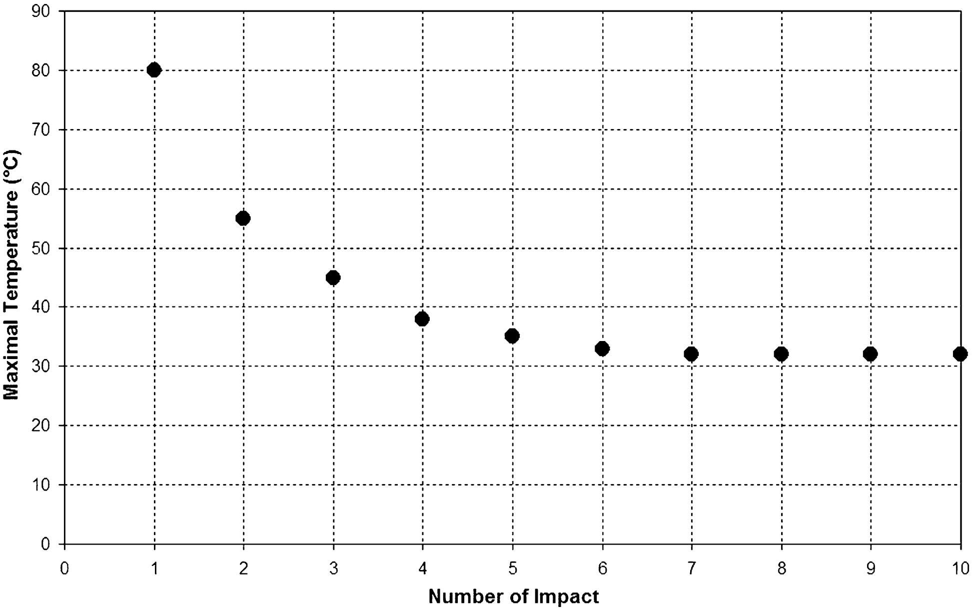

Fig. 4. Maximal temperature reached in the steel during an impact as a function of the number of impact.

no evidence of dynamic effects, except on the indenter kinematics [17]. This hypothesis is valid if the impact time is much higher than the elastic wave propagation in the region of contact [18]. This last condition can be written:

$$t_{\text{impact}} > \frac{2a}{c}$$

where t_{impact} is the impact time, a is the maximum contact radius and c is the longitudinal elastic wave speed in the sample. In our experiment the contact duration is about 200 μs whereas the ratio a/c is about 100 ns. The main problem with such approach is that the indenter kinematics is not known a priori and should change at each impact. The algorithm we developed to simulate normal energy controlled impact is based on the energy balance. During one impact the penetration depth increases until the work produced by the indentation equals the kinetic energy. Then the penetration depth decreases until the material is fully unloaded. Thanks to this algorithm more than two thousand impacts can be simulated in less

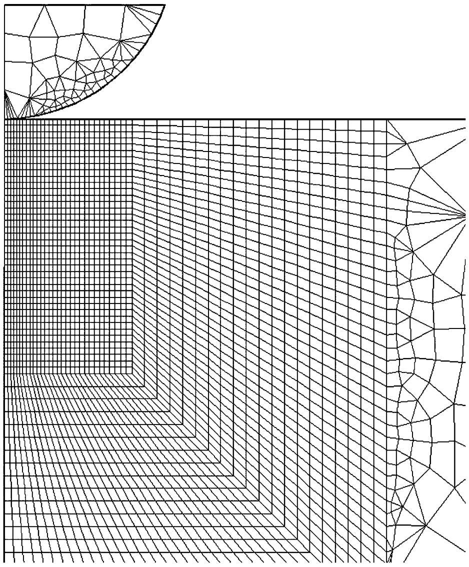

Fig. 5. Finite element mesh.

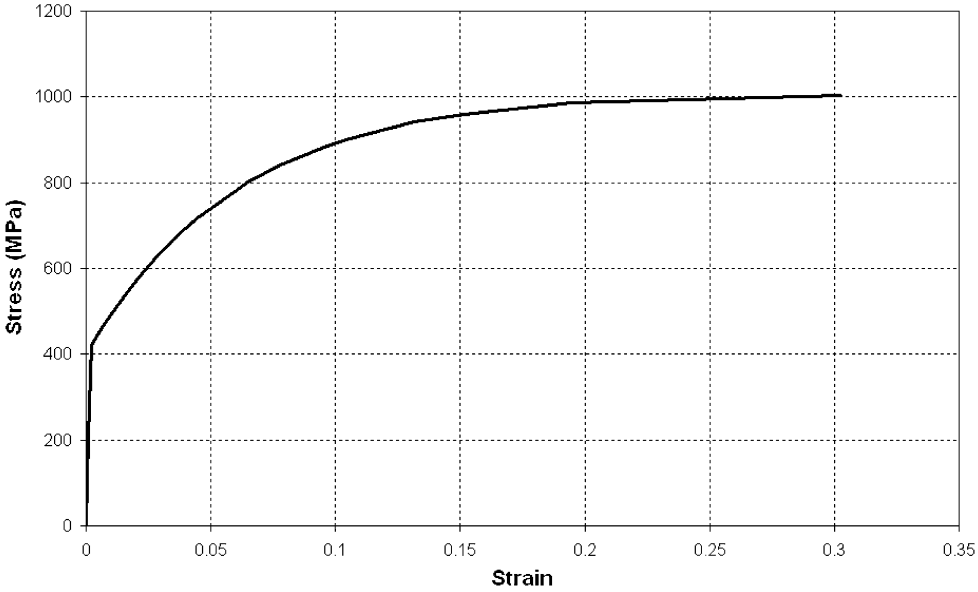

Fig. 6. Stress–strain curve of the AISI1045 steel (compression test).

than two days on a Pentium 4 – 3.6 GHz – RAM 2 Go. This algorithm has been implemented in the finite element software Systus [19].

Calculations have been performed using axisymmetric elements and a large displacement/large strain option (updated Lagrangian formulation). The mesh is specially refined near the contact zone, but is also sufficiently wide to approximate a semi-infinite solid (Fig. 5). The contact between the indenter and the workpiece is frictionless and loading is achieved by imposing a quasi-static displacement of the indenter as explained above. The indenter is assumed to be perfectly rigid and the contact between the ball and the surface is frictionless. In order to ensure plastic incompressibility, four node quadrilateral isoparametric elements with a selective reduced integration scheme are used in the plastically deformed area.

3.3. Materials

According to the literature, MAS are consequences of severe plastic deformation induced by the repeated impacts [5–9]. Hence the modeling of such a phenomenon requires one to identify the mechanical behavior at very large strain of the AISI1045 steel. Moreover it is well known that the elastic–plastic properties of such a steel will depend on the high strain rate induced by the impact. In absence of such data, we have used the stress–strain curve plotted in Fig. 6 in the finite

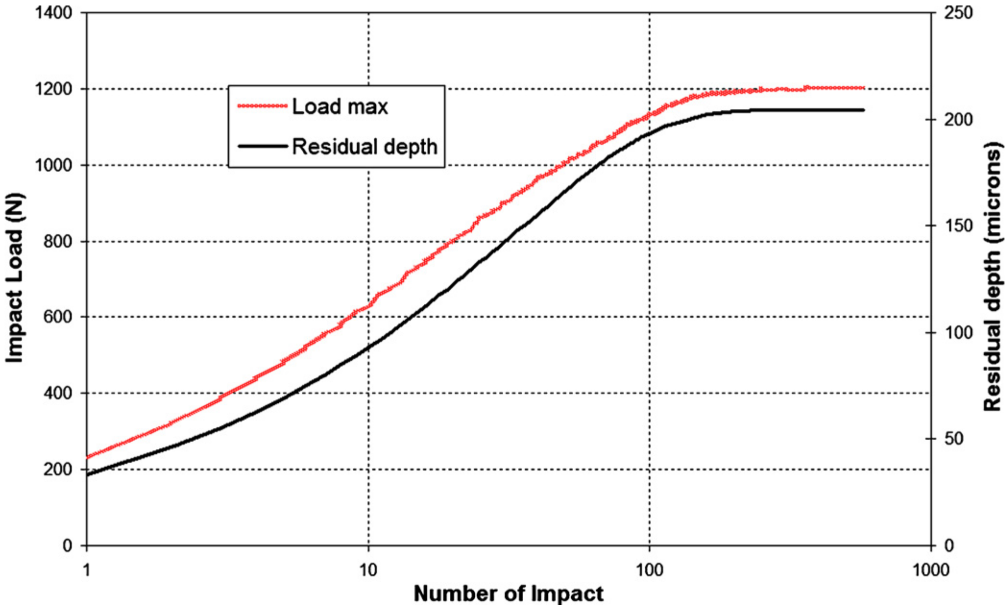

Fig. 7. Evolution of the penetration depth and the impact load as a function of the number of impacts (FEA results).

element model. This last has been measured using a classical compression testing device at low strain rate and at ambient. Let us observe that the saturation of the strain hardening seems to occur for a plastic strain about 30%. The aim of this study being to investigate phenomenologically the growth of the mechanically attrited structure under repeated impact, we have not tried to identify a more suited stress–strain curve. The plastic flow is described via a classic von Mises elastic–plastic model with pure isotropic strain hardening.

4. Finite element investigation

4.1. Transient and stabilized impact regimes

The transient impact regime is characterized by a growth of the residual print at each impact. In Fig. 7, the depth of the residual print is plotted as a function of the number of impact. The stabilization of the residual depth is observed after 150 impacts, which correspond to the beginning of the stabilized impact regime. Indeed the structure shakedown to a macroscopic elastic response. There is no more increase of the contact area per impact. This result is also in good agreement with Sekkal et al. [1] experiments. The depth of the indent print is around 200 μm when the stabilized regime is reached. This phenomenon is close to the process of cumulative plastic deformation under repeated rolling [20], whereby plastic deformation introduces residual stresses which make the steady elastic cyclic state virtually reached after a given number of cycles. The evolution of the maximum load per impact follows the same trend. In the stabilized impact regime, the impact load is about 1200 N which is in good agreement with the load measured by the micro-impact tester sensor (about 1100 N).

4.2. Plastic strain distribution

The main interest of finite element modeling is that it allows to access to physical quantities which are difficult and costly to measure experimentally, such as plastic strains. In metal plasticity, the history of plastic deformation is often characterized by the cumulated plastic strain:

$$p = \int_0^t \dot{\varepsilon}_{eq}^p \, \mathrm{d}\tau \quad \text{where } \dot{\varepsilon}_{eq}^p = \sqrt{\frac{2}{3}\dot{\varepsilon}_{ij}^p \dot{\varepsilon}_{ij}^p}$$

The cumulated plastic strains obtained after 200 impacts and after 2000 impacts are plotted in Fig. 8. Both cases are in the stabilized impact regime, thus the macroscopic response of the material should be elastic. For both impacts, the maximum value of cumulated plastic strain is located just under the surface in the zone where the transformed structure should appear. Nevertheless it is shown that the cumulated plastic strain distributions are significantly different. Indeed, the plastic deformation is more severe after 2000 impacts than after 200 impacts. It points out that although the macroscopic response is elastic during the stabilized impact regime, there is still a zone where a plastic flow occurs.

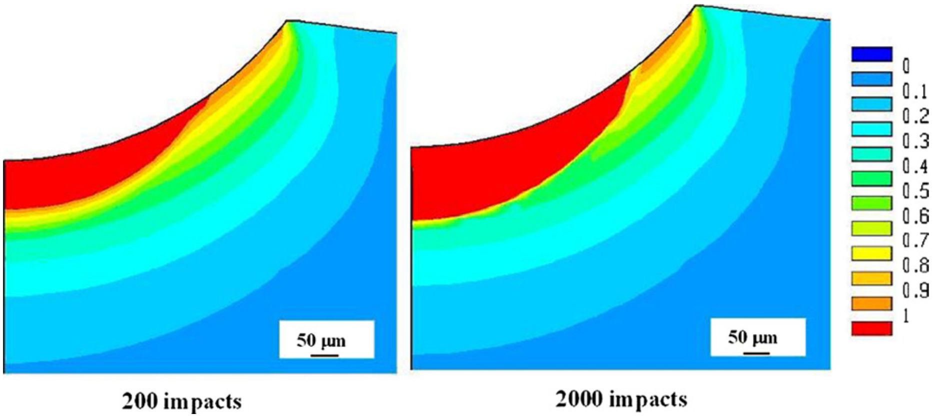

Fig. 8. Distribution of cumulated plastic strain p after 200 and 2000 impacts. In the red zone, the cumulated plastic strain is up to 1.

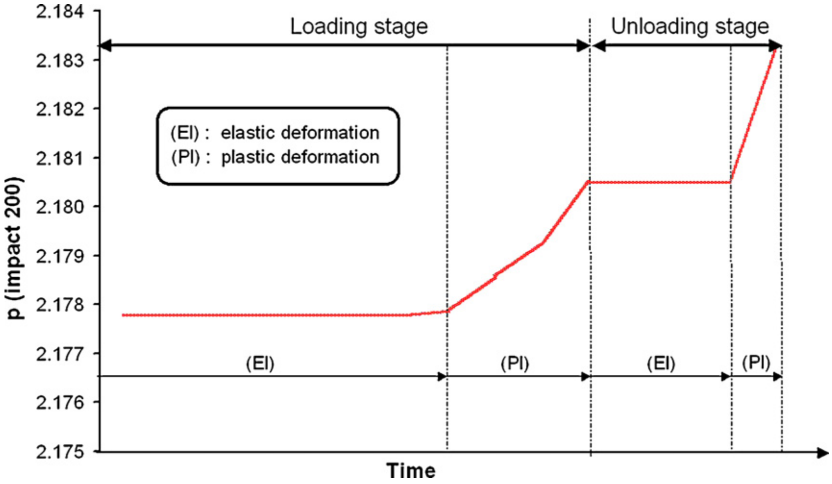

Fig. 9. Evolution of the cumulated plastic strain during the 200th impact. An equivalent amount of cumulated plastic strain is produced during the loading stage and during the unloading stage.

Let us observe what happens at a point M located 100 µm below the surface (observed transformed zone) during one impact (Fig. 6). During the loading, the point M behaves elastically until the plastic criterion is satisfied. Then plastic flow occurs. A small increase of plastic deformation has been produced in this point during the loading part. During the unloading (rebound of the ball), the elastic deformations recover. Nevertheless, at the end of the unloading, a complex residual stress state exists due to the previous plastic strain. Because of this stress state, the plastic criterion may be satisfied and reversed plastic deformation may take place. Indeed, a close examination of the plastic flow reveals that the material is first sheared in one direction during the loading part then sheared in the opposite direction during the unloading stage. Fig. 9 shows that an equivalent amount of cumulated plastic strain is produced during the loading and unloading stages. The plastic strain created during the loading is like "recovered" during the unloading. The material in the stabilized impact regime is thus submitted to a reversal plastic deformation. Orlov et al. [21] have shown that strain reversal may also lead to plastic strain induced grain refinement, although it retarded this phenomenon compared to monotonic deformation.

One consequence of this reversal plastic deformation is that the geometry before an impact in the stabilized impact regime is similar to the geometry after. This is the reason why an impact in the stabilized impact regime appears to be macroscopically elastic whereas the cumulated plastic strain increases at each impact in the mechanically transformed structure.

5. Modeling the creation and the growth of the MAS

5.1. A new mechanism

Sekkal et al. have shown that the MAS they observed was composed of nanocrystalline structure (grain size about 30–100 nm). The mechanically transformed structure obtained in the present study on the AISI1045 steel has the same features than the MAS of Sekkal et al. [1], thus it should be also composed of nanograins. The FEA reveals that the zone

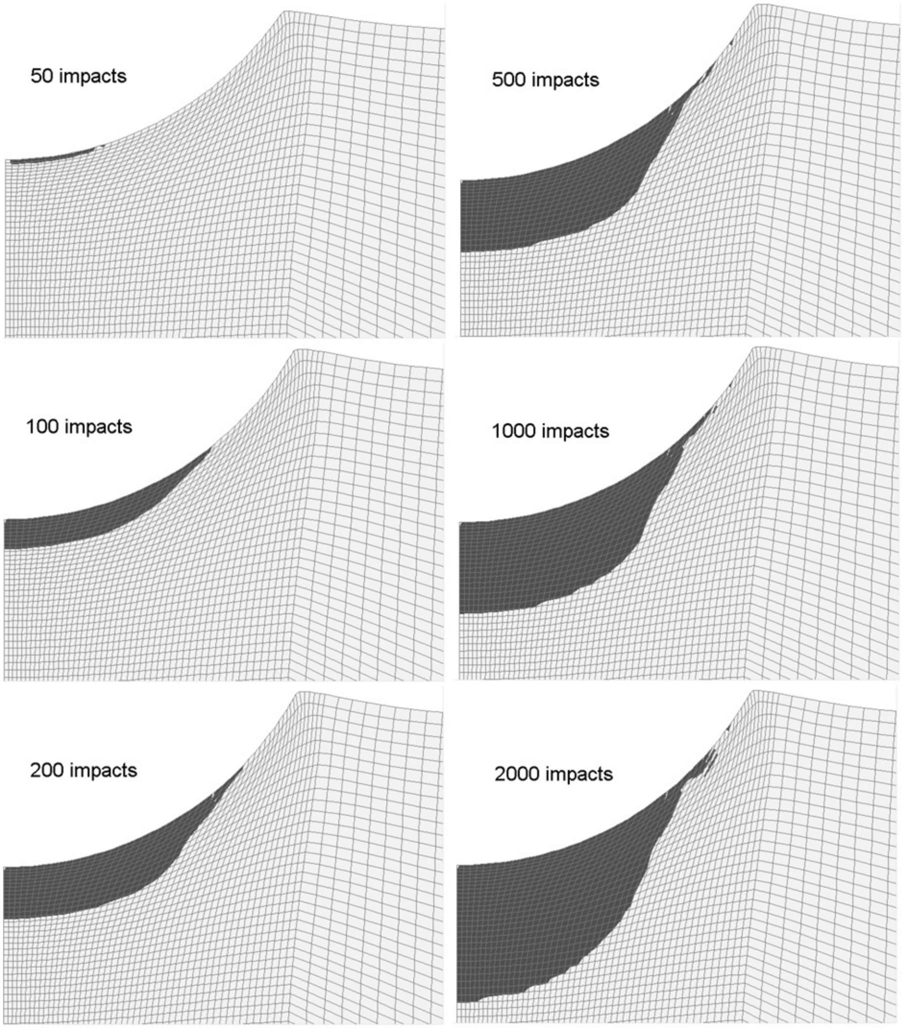

Fig. 10. Evolution of the Mechanically Attrited Structure (MAS) as a function of the number of impact. The MAS is in black color. The plastic strain threshold before transformation of the microstructure is here $p_{\mathrm{crit}} = 150\%$.

where severe plastic deformations occur is inside the zone where the MAS has been experimentally observed. In this zone, the cumulated plastic strain increases at each impact and can reach very important values. This cumulative plastic deformation during the stabilized impact regime can be viewed as a local mechanical mixing of the material. As suggested by Lu et al. [6–9], the plastic strain induced grain refinement process under impact conditions is due to the combination of the large plastic strain reached locally and the high strain rates induced by the impacts (between 100 s^{-1} and 1000 s^{-1}). Hence, when plastic deformation reaches a given value, nanocrystalline structures may be created. The MAS is very hard, thus, it will act as a new indenter on the region below, which will also be transformed into an MAS following the same mechanism. Consequently MAS should grow progressively, starting from the surface.

5.2. Finite element modeling

This mechanism has been implemented in the FE model developed previously: When the cumulated plastic strain p inside a finite element exceeds a critical value p_{MAS}, the element is transformed into an MAS. The MAS is assumed as a perfectly linear elastic solid with the same properties than those of the initial AISI1045 steel. The plastic strain threshold before the transformation of a point into an MAS being unknown, an arbitrary value of $p_{\mathrm{MAS}} = 150\%$ has been chosen.

The growth of the MAS is represented in Fig. 10. During the transient impact regime (impact number < 150), the contact area increases at each impact. When the stabilized impact regime is reached, the geometry of the contact remains constant, but the plastic deformation just under the indenter continues to increase until it reaches the critical value of 150%. Then the created MAS acts as a new indenter on the material below. After a given number of cycle, the material below is transformed into a new MAS and acts as a new indenter. The shape of the MAS created is very close to the observed experimental shape

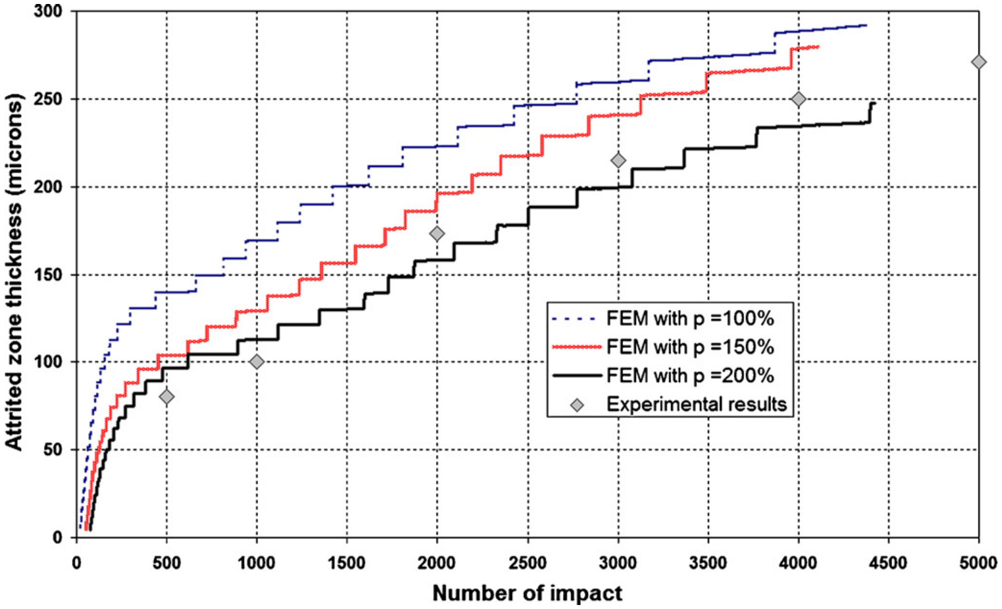

Fig. 11. Evolution of the MAS thickness as a function of the number of impacts for different values of p_{crit}. The best agreement between the FE results and the experimental results corresponds to $p_{\text{crit}} = 200\%$.

(Fig. 2). According to this mechanism, the MAS grows during the transient impact regime and also during the stabilized impact regime.

The kinetics of the MAS growth (MAS thickness vs number of impacts) is plotted in Fig. 11 for different values of the plastic strain threshold: $p_{\text{MAS}} = 100\%$, $p_{\text{MAS}} = 150\%$ and $p_{\text{MAS}} = 200\%$. From a qualitative point of view, the kinetics of the MAS growth is well reproduced. The best agreement is obtained with $p_{\text{MAS}} = 200\%$. During the first 500 impacts, the MAS grows rapidly until it reaches a thickness of 100 μm. As shown in Fig. 10, the MAS grows both in the radial direction (length) and in the impact direction (thickness). After 500 impacts, the MAS length is stabilized. Only its thickness increases until it reaches a maximum value of about 300 μm (after 3000 or 5000 impacts depending the value of p_{crit}) which is in good agreement with the experimental results.

6. Conclusion

From the finite element analyses presented above, two domains, corresponding to different responses of the tested material under repeated energy controlled normal impacts, have been identified:

The first one corresponds to the transient impact regime and is characterized by high plastic deformations. During this regime there is an important increase of the contact area and of the penetration depth and the subsurface is strongly cold hardened.

The second one corresponds to the stabilized impact regime, reached approximately after 150 cycles. It results from a plastic accommodation [17] due to the increase of the contact area per impact. The structure shakedown to a perfectly elastic response and the residual penetration depth remains constant. Nevertheless, it appears that plastic yielding occurs in the zone where the mechanically attrited structure should be created. In this zone, the cumulated plastic strain may increase indefinitely whereas the neighborhood undergoes only elastic deformations. When the plastic deformation is large enough (after a number of cycles which depend on the kinetic energy of the ball), this zone can be changed into an MAS. These observations lead us to propose the following mechanism, which has been implemented in the finite element software Systus:

The first amount is created after a given number of cycles when a critical value of the cumulated plastic deformation is reached (plastic shakedown). The MAS is very hard, thus, it acts as a new indenter on the region below, which will also be transformed into an MAS following the same mechanism. Consequently MAS grows progressively, starting from the surface. In our opinion, the MAS induced by repeated impacts is mainly due to a cyclic plastic shearing of the material just under the indenter during the stabilized impact regime.

The main parameters governing the formation of MAS zones seem thus to be the number of cycles and also the kinetic energy of the indenter. Indeed, the higher the kinetic energy, the higher the contact area during the stabilized impact regime, and thus the higher should be the size of the MAS. It has been shown that the rise of temperature during one impact is not high enough to induce alone structural changes in the material. Nevertheless, the temperature has to be high enough to ensure that the material could undergo severe plastic deformation. The main effect of the high hydrostatic pressure is also to ensure that the material could undergo this severe plastic deformation in preventing damaging phenomena.

This work is a first step to understand the process parameters responsible of the growth of mechanically attrited structures under more complex impact loadings such as impacts occurring during shot peening processes. Future works will deal with the influence of impact angles and friction properties.

References

[1] A.C. Sekkal, C. Langlade, A.B. Vannes, Tribologically transformed structure of titanium alloy (tial6v4) in surface fatigue induced by repeated impacts, Materials Science and Engineering A 393 (1–2) (2005) 140–146.

[2] J.E. Morgan, Structural and microstructural changes in the inner races of ball bearings, Wear 84 (1) (1983) 51–64.

[3] E. Sauger, L. Ponsonnet, J.M. Martin, L. Vincent, Study of the tribologically transformed structure created during fretting tests, Tribology International 33 (11) (2000) 743–750.

[4] M. Umemoto, Y. Todaka, J. Li, K. Tsuchiya, Nanocrystalline structure in steels produced by various severe plastic deformation processes, Materials Science Forum 503–504 (2006) 11–18.

[5] G. Kermouche, A.L. Kaiser, P. Gilles, J.M. Bergheau, Combined numerical and experimental approach of the impact-sliding wear of a stainless steel in a nuclear reactor, Wear 263 (2007) 1551–1555.

[6] K. Lu, J. Lu, Nanostructured surface layer on metallic materials induced by surface mechanical attrition treatment, Materials Science and Engineering A 375–377 (2004) 38–45.

[7] N.R. Tao, Z.B. Wang, W.P. Tong, M.L. Sui, J. Lu, K. Lu, An investigation of surface nanocrystallization mechanism in Fe induced by surface mechanical attrition treatment, Acta Materialia 50 (2002) 4603–4616.

[8] H.W. Zhang, Z.K. Hei, G. Liu, J. Lu, K. Lu, Formation of nanostructured surface layer on AISI 304 stainless steel by means of surface mechanical attrition treatment, Acta Materialia 51 (2003) 1871–1881.

[9] H. Chan, H. Ruan, A. Chen, J. Lu, Optimization of the strain rate to achieve exceptional mechanical properties of 304 stainless steel using high speed ultrasonic surface mechanical attrition treatment, Acta Materialia 58 (2010) 5086–5096.

[10] M. Busquet, S. Descartes, Y. Berthier, Formation conditions of mechanically modified superficial structures for two steels, Tribology International 42 (2009) 1730–1743.

[11] D.A. Rigney, L.H. Chen, M.G.S. Naylor, A.R. Rosenfield, Wear processes in sliding systems, Wear 100 (1984) 195–219.

[12] C. Suryanarayana, E. Ivanov, V.V. Boldyrev, The science and technology of mechanical alloying, Materials Science and Engineering A 304–306 (2001) 151–158.

[13] S. Lamri, C. Langlade, G. Kermouche, V. Martinez, Estimation of the stress relief induced in CrN thin films by buckling, Materials Science and Engineering A 527 (2010) 7912–7919.

[14] A. Sekkal, C. Langlade, A.B. Vannes, A micro/macro impact test at controlled energy for erosion and phase-transformation simulation, Tribology Letters 15 (3) (2002) 265–274.

[15] Abaqus User's Manual, Abaqus Inc., 2009.

[16] S.P. Jaspers, J.H. Dautzenberg, Material behavior in conditions similar to metal cutting: flow stress in the primary shear zone, Journal of Materials Processing Technology 122 (2002) 322–330.

[17] K.L. Johnson, Contact Mechanics, Cambridge University Press, Cambridge, UK, 1985.

[18] J.P. Nobre, A.M. Dias, R. Gras, Resistance of a ductile steel surface to spherical normal impact indentation: use of a pendulum machine, Wear 211 (1997) 226–236.

[19] Systus/Sysweld, User's Manual, ESI Group, 2004.

[20] K.L. Johnson, Contact mechanics and the wear of metals, Wear 190 (1995) 162–170.

[21] D. Orlov, Y. Todaka, M. Umemoto, T. Nobuhiro, Role of strain reversal in grain refinement by severe plastic deformation, Materials Science and Engineering A 499 (2009) 427–433.